ELSEVIER

Journal of Alloys and Compounds 452 (2008) 406–409

Journal of ALLOYS AND COMPOUNDS

www.elsevier.com/locate/jallcom

Lanthanum zirconate ceramic toughened by $BaTiO_3$ secondary phase

J.Y. Li [a,b], H. Dai [a,b], X.H. Zhong [a,b], Y.F. Zhang [a,b], X.F. Ma [a], J. Meng [a], X.Q. Cao [a,*]

[a] *Key Lab of Rare Earth Chemistry and Physics, Changchun Institute of Applied Chemistry,*
Chinese Academy of Sciences, Changchun 130022, Jilin, China
[b] *Graduate School of the Chinese Academy of Sciences, Beijing 100049, China*

Received 8 October 2006; accepted 3 November 2006
Available online 18 December 2006

Abstract

$La_2Zr_2O_7$ (LZ) is a promising thermal barrier coating material for the high-temperature applications, which could be significantly toughened by the $BaTiO_3$ piezoelectric phase incorporated into the matrix. The composites of xBaTiO$_3$/(1 − x)LZ (x = 5, 10, 15, 20 vol%, LZ-x-BaTiO$_3$) were densified by means of high-pressure sintering (HPS) under a pressure of 4.5 GPa at 1450 °C for 10 min, by which a high relative density above 93% could be obtained. The morphologies of the fractured surfaces were investigated by the scanning electron microscope, and the fracture toughness and Vicker's hardness of the composites were evaluated by the microindentation. The grain size of the LZ matrix drops significantly with the addition of $BaTiO_3$ piezoelectric phase and the fracture type changes from the intergranular to a mixture type of the transgranular and intergranular in the composites. The LZ-10-BaTiO$_3$ composite has a fracture toughness of 1.98 MPa m$^{1/2}$, which is obviously higher than that of the pure LZ (1.60 MPa m$^{1/2}$), and the toughening mechanism might be attributed to the ferroelastic domain switching of ferroelectric phase $BaTiO_3$.

Keywords: Ceramic; Piezoelectricity; Mechnical properties; High-pressure

1. Introduction

Thermal barrier coatings (TBCs) have found an increasing number of applications in protecting high-temperature metallic components, for example, TBCs are deposited on transition pieces, combustion lines, first-stage blades and vanes, and other hot-path components of gas turbines either to increase the inlet temperature with a consequent improvement of the efficiency or to reduce the requirements for a cooling system [1]. There are several ceramics that have been evaluated as TBC materials [2], and lanthanum zirconate is one of the most promising among them [2–8]. The properties of high melting point, phase-stability up to its melting point, low thermal conductivity, low sintering ability and oxygen-nontransparent are the major reasons that it is believed to have potential as TBC material for high-temperature applications. However, its practical applications are limited by the low fracture toughness. The brittleness of ceramics is the common problem, which restricts ceramics from the application in fields where high strength and toughness are required.

In recent decades, a variety of approaches to improve the fracture toughness of ceramics have been developed, and the toughening mechanisms include the phase transformation, microcracking, nanofication, fiber/whisker reinforcement, grain bridging, etc. [9–13], which are all based on the energy dissipation and energy balance approach [14]. Recently, a new approach for toughening of ceramics, which introduces some piezoelectric secondary phase into the matrix, has been proposed and investigated [15–18]. Toughening is achieved through energy dissipation due to the piezoelectric effect or/and domain wall motion. The systems such as $Sr_2Nb_2O_7$/3Y-TZP [16], $Nd_2Ti_2O_7/Al_2O_3$ [17] and $BaTiO_3$/3Y-TZP [18] composites had been studied and the fracture toughness of matrixes showed a significant increase.

As the first ferroelectrics ceramic, $BaTiO_3$ is widely used as capacitor, sensor and actuator. Recently, *R*-curve behavior due to stress-induced ferroelastic domain switching was also found in $BaTiO_3$ ceramic [19]. Moreover, the effect of $BaTiO_3$ piezoelectric phase on the fracture toughness of Al_2O_3 ceramic had been presented by Zhan et al. [15] and the improvement of fracture toughness had been achieved. The anisotropy behavior in crack propagation is observed in the poled $BaTiO_3/Al_2O_3$ composite [20], indicating that the domain

---

[*] Corresponding author.
E-mail address: xcao@ciac.jl.cn (X.Q. Cao).

0925-8388/$ – see front matter © 2006 Elsevier B.V. All rights reserved.
doi:10.1016/j.jallcom.2006.11.025

switching plays an important role in the toughness variation of composite.

In the present work, the composites of LZ-x-$BaTiO_3$ had been densified by high-pressure sintering (HPS) method and the fracture toughness was investigated by Vickers indentation technique.

2. Experimental

The LZ powder was synthesized by solid-state reaction using La_2O_3 (99.99%) and ZrO_2 (99.6%). Starting materials were ball-milled for 24 h in distilled water with zirconia balls. The mixture was heated at 1400 °C for 12 h and ball-milled again. The $BaTiO_3$ was prepared by sol–gel method: the $Ba(AC)_2$ dissolved in distilled water was added dropwise to a prepared solution of stoichiometric amounts of tetra-*n*-butyl titanate in isopropanol under stirring. The gelation was initiated after stirring for 30 min and the LZ powder was dispersed in this gel. The mixture was dried at 80 °C for 24 h and subsequently calcinated at 800 °C for 12 h to synthesize the LZ-x-$BaTiO_3$ composites. Small pieces of round-shape samples with a diameter of 11 mm were obtained by pressing LZ-x-$BaTiO_3$ composites powders under a pressure of 0.3 GPa at room temperature. For the indentation test, such small pieces were further densified by HPS under a pressure of 4.5 GPa at 1450 °C for 10 min (6 × 800 Ton 6-Axial Presser, The Prospect Machine Factory of Hebei Zhang Jia Kou).

X-ray diffraction (XRD) patterns were collected on a Rigaku D/Max-IIB diffractometer with Cu Kα radiation (0.15406 nm). Density was measured by the Archimedes method in distilled water. The morphologies of the composites and the microstructures of the densified samples were analyzed by the scanning electron microscope (SEM, XL 30 ESEM FEG, Micro FEI Philips). Before the indentation test, the surfaces of the densified samples were polished with diamond suspensions (Metadi Diamond 15–1 μm, Buehler) by a low-speed automatic polisher (Minimet 1000, Buehler). The fracture toughness and Vicker's hardness were measured by a microindentor (FM-700, Future-Tech) with a load of 3 N for 15 s.

3. Results and discussion

The XRD patterns of LZ-x-$BaTiO_3$ composites powders after calcination at 800 °C are shown in Fig. 1 and the phase constitutions can be clearly confirmed by the results of XRD analysis. The major peaks are in agreement with those of the JCPDS cards LZ (No. 17-0450) and $BaTiO_3$ (No. 03-0725), and the intensities of $BaTiO_3$ peaks are increased with the increase of $BaTiO_3$ volume content. The LZ-x-$BaTiO_3$ composites are densified by HPS under a pressure of 4.5 GPa at 1450 °C for 10 min and the XRD pattern of the LZ-10-$BaTiO_3$ composite is shown in Fig. 2. After densification by HPS, the LZ and $BaTiO_3$ would remain as the major phases and the intensities of $BaTiO_3$ and LZ peaks have no obviously change. There is no impurity phase is detected in densified sample, indicating that the HPS process does not produce a reaction between the LZ and $BaTiO_3$ phases. In regard to piezoelectric toughening mechanism, it is important to prevent the piezoelectric phase from reacting with the matrix. The HPS process with such a high pressure and a short sintering time is an effective sintering method for preventing the reaction happening.

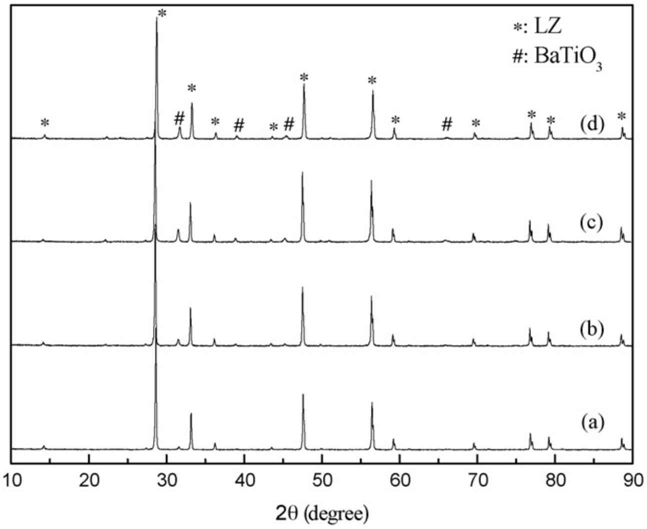

Fig. 1. The XRD patterns of LZ-x-$BaTiO_3$ composites powders: (a) $x = 5$ vol%; (b) $x = 10$ vol%; (c) $x = 15$ vol%; (d) $x = 20$ vol%.

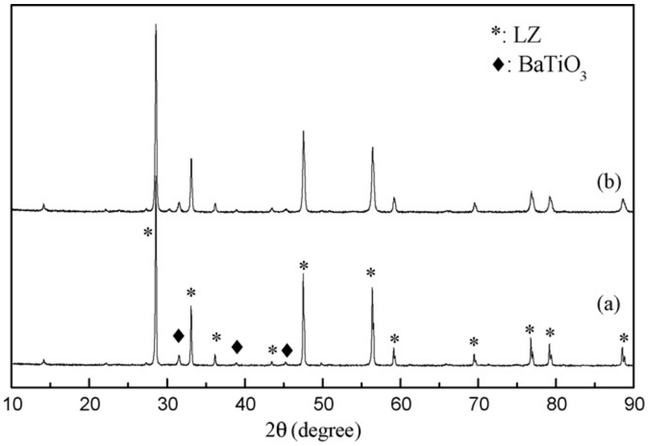

Fig. 2. The XRD patterns of LZ-10-$BaTiO_3$ composite: (a) powders calcinated at 800 °C for 12 h; (b) sample densified by HPS at 1450 °C for 10 min.

The microstructures of the fractured surfaces of the pure LZ and LZ-x-$BaTiO_3$ composites densified by HPS are shown in Fig. 3. The fracture type of the pure LZ is found to be intergranular, while the composites exhibit a mixture of the transgranular and intergranular fracture. On the other hand, the micrographs of fracture surfaces also indicate that the grain size of the LZ matrix drops significantly with the addition of $BaTiO_3$ particles. The average grain sizes of LZ matrix evaluated from SEM images are shown in Table 1. The grain size of the pure LZ densified by HPS is about 1 μm, while that of the LZ-10-$BaTiO_3$ composite is less than 0.3 μm. It is attributed to that the $BaTiO_3$ particles, which are dispersed in the LZ matrix, restrict the grain boundary movement and limit the grain growth of the LZ matrix during the HPS process [21].

Table 1
Physical properties of the LZ and LZ-x-$BaTiO_3$ composites in this study

$BaTiO_3$ content (vol%)	Relative density (%)	Hardness (GPa)	Mean LZ grain size (μm)
0	93.7	10.54	1
5	95.7	10.21	0.5
10	96.6	10.63	0.3
15	97.9	10.57	–
20	92.5	10.53	–

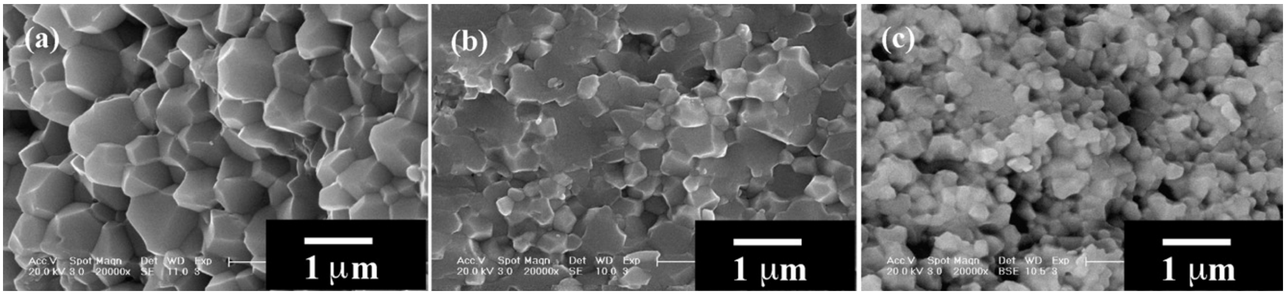

Fig. 3. SEM images of the fracture surfaces of LZ and LZ-x-BaTiO$_3$ composites prepared by HPS: (a) LZ; (b) $x = 5$ vol%; (c) $x = 10$ vol%.

From the Table 1, it can be noted that all the composites densified by HPS have a high relative density above 93%. The relative density is increased with the increase of BaTiO$_3$ content, which is attributed to the addition of BaTiO$_3$ powder. It is reported in Ref. [9] that the grain growth can restrict the density increase during sintering when it outweighed the density increase. The addition of BaTiO$_3$ powder limits the grain growth of LZ matrix during sintering, which is obviously observed in SEM images, and increases the relative density. The other reason for the density increase is that the addition of BaTiO$_3$ with low melt point (1705 °C), which lowers the liquid phase formation temperature of the system and increases the liquid content, is helpful for the sintering. When the volume content of BaTiO$_3$ is 15 vol%, the relative density shows a maximum value of approximately 98%. For situation of high concentration of BaTiO$_3$ ($x > 15$ vol%), the density reduction is observed in LZ-20-BaTiO$_3$ composite. Due to the difference of thermal expansion coefficients (TECs) for BaTiO$_3$ and LZ, the incorporation of pores into the matrix grains leads to the forming of macrocracks during cooling after sintering and the decreasing of density during sintering.

Vicker's hardnesses of the composites were measured at room temperature and the results were shown in Fig. 4. The fracture toughness (K_{IC}) is estimated from the crack length [22]:

$$K_{\mathrm{IC}} = 0.16 H a^{1/2} (c/a)^{-3/2}$$

where H is hardness, $2c$ the crack and impression length and $2a$ is the length of the indent diagonal. It is observed that the fracture toughness K_{IC} of LZ matrix is significantly improved by incorporating a modest amount of BaTiO$_3$ piezoelectric phase and the maximum fracture toughness of 1.98 MPa m$^{1/2}$ is achieved for the composite of LZ-10-BaTiO$_3$. The stress-induced domain switching process near the crack tip due to the high tensile stress is used to explain the enhanced toughness of the LZ-x-BaTiO$_3$ composites. The R-curve behavior of BaTiO$_3$, which is produced by stress-induced ferroelastic domain switching, has been presented by Meschke et al. [19] and the toughness mechanism is similar to that for phase transformation toughening in zirconia-toughened ceramics. Both of the toughening mechanisms are based on the energy dissipation and energy balance approach. In zirconia-toughened ceramics, the transformation with volume dilation of 5 vol% is stress-induced near the crack tip and results in compressive stress [23]. When the crack extends, this compressive stress act on the crack wake and cause shielding of the crack tip from the applied load. Similarly, for the LZ-x-BaTiO$_3$ composites, the toughening mechanism is the domain switching induced by high tensile stress around the crack tip. In the unpoled composites samples, the domain orientations of BaTiO$_3$ are random. When the crack extends, the stress induces polar rotation of domain and causes compressive stress. Just as in the case of zirconia-toughened ceramics, this stress can cause shielding of crack tip through energy dissipation [24]. The above discussions indicate the significant toughening effect when a suitable piezoelectric phase is introduced into matrix. For the higher BaTiO$_3$ concentration (>10 vol%), the toughening effect is limited by the increased residual stress and the macrocracks, which are formed during cooling after sintering due to the different TECs of LZ and BaTiO$_3$. The effect of the addition of BaTiO$_3$ on Vicker's hardness is not obvious and the hardness values of LZ-x-BaTiO$_3$ composite materials are closed to that for LZ matrix.

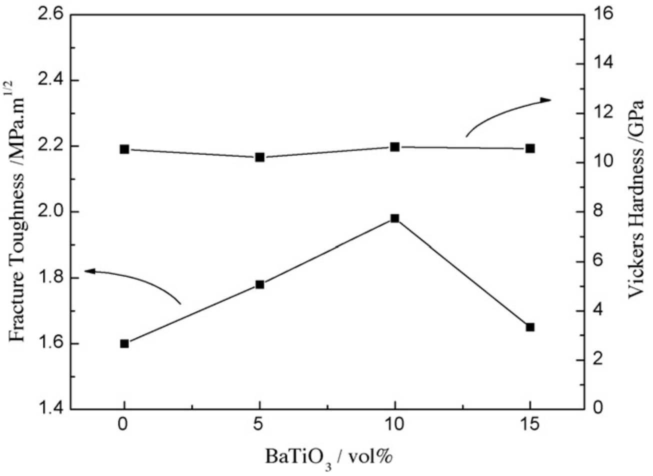

Fig. 4. Fracture toughness and Vicker's hardness of LZ-x-BaTiO$_3$ composites.

4. Conclusion

The study of this work indicates that the HPS with such a high pressure for a short period is a good choice for the sintering of LZ-x-BaTiO$_3$ composites, and the addition of BaTiO$_3$ piezoelectric secondary phase is really an efficient way for the improvement of fracture toughness.

Acknowledgement

This work was financially supported by the project of NSFC-20471058.

References

[1] F. Cernuschi, P. Bianchi, M. Leoni, P. Scardi, J. Therm. Spray Technol. 8 (1999) 102–109.

[2] X.Q. Cao, R. Vassen, D. Stoever, J. Eur. Ceram. Soc. 24 (2004) 1–10.

[3] R. Vassen, X. Cao, F. Tietz, in: E., Lugscheider, P.A., Kammer (Eds.), Proceedings of the United Thermal Spray Conference'99, Duesseldorf Germany, March, 1999, ASM International, Verlag fuer Schweissen und Verwandte Verfahren, Duesseldorf, 1999, pp. 830–834.

[4] R. Vassen, X. Cao, F. Tietz, D. Basu, D. Stoever, J. Am. Ceram. Soc. 83 (2000) 2023–2028.

[5] X.Q. Cao, R. Vassen, W. Jungen, S. Schwartz, F. Tietz, D. Stoever, J. Am. Ceram. Soc. 84 (2001) 2086–2090.

[6] R. Vassen, F. Tietz, G. Kerkhoff, D. Stoever, in: J., Lecomte-Beckers, F., Schuber, P.J., Ennis (Eds.), Proceedings of the 6th Liege Conference on Materials for Advanced Powder Engineering, Universite de Liege, Belgium, November, 1998, Forschungszentrum Juelich GmbH, Deutschland, 1998, pp. 1627–1635.

[7] R. Vassen, X.Q. Cao, M. Dietrich, D. Stoever, in: Mrityunjay Singh, Tpdd Jessen (Eds.), Proceedings of the 25th Annual International Conference on Advanced Ceramics and Composites: An Advanced Ceramics Odyssey, Cocoa Beach of Florida, January 2001, Am. Ceram. Soc., 2001, pp. 435–443.

[8] J. Michael Maloney, Thermal Barrier Coating Systems and Materials, European Patent EP 0848077 Al, 1998.

[9] H.Y. Lee, W. Riehemann, B.L. Mordike, J. Eur. Ceram. Soc. 10 (1992) 245–253.

[10] G. Grathwohl, A. Hahnel, B. Meier, E. Pippel, G. Richter, J. Woltersdorf, J. Eur. Ceram. Soc. 10 (1992) 1–12.

[11] R.H.J. Hannink, P.M. Kelly, B.C. Muddle, J. Am. Ceram. Soc. 83 (2000) 461–487.

[12] F.F. Lange, J. Mater. Sci. 17 (1982) 235–239.

[13] J. Karch, R. Birringer, H. Gleiter, Nature 330 (1987) 556–558.

[14] A.G. Evans, J. Am. Ceram. Soc. 73 (1990) 187–206.

[15] G.D. Zhan, J. Kuntz, J. Wan, J. Garay, A.K. Mukherjee, Mater. Sci. Eng. A 356 (2003) 443–446.

[16] X.M. Chen, X.Q. Liu, F. Liu, X.B. Zhang, J. Eur. Ceram. Soc. 21 (2001) 477–481.

[17] B. Yang, X.M. Chen, J. Eur. Ceram. Soc. 20 (2000) 1687–1690.

[18] B. Yang, X.M. Chen, X.Q. Liu, J. Eur. Ceram. Soc. 20 (2000) 1153–1158.

[19] F. Meschke, A. Kolleck, G.A. Schneider, J. Eur. Ceram. Soc. 17 (1997) 1143–1149.

[20] S. Rattanachan, Y. Miyashita, Y. Mutoh, J. Eur. Ceram. Soc. 24 (2004) 775–783.

[21] H.J. Hwang, T. Nagaai, M. Sando, M. Toriyama, K. Niihara, J. Eur. Ceram. Soc. 19 (1999) 993–997.

[22] A.G. Evans, E.A. Charles, J. Am. Ceram. Soc. 7–8 (1976) 371–372.

[23] R.W. Steinbrech, J. Eur. Ceram. Soc. 10 (1992) 131–142.

[24] G.A. Schneider, V. Heyer, J. Eur. Ceram. Soc. 19 (1999) 1299–1306.